

# **Inherently dissipative normal currents during thermodynamic changes of state in superconductors: Joule heating vs. magnetocaloric cooling**

Andreas Schilling

*Dept. of Physics, University of Zürich, 8057 Zürich, Switzerland*

*Email: andreas.schilling@physik.uzh.ch*

**In the Meissner phase of a superconductor below its critical temperature, an external constant magnetic field is shielded by circulating persistent supercurrents with zero resistance that are formed by Cooper pairs. However, a thermodynamic change of state within this phase at any finite temperature and at finite speed, such as a cooling or a heating, inevitably generates normal currents of thermally excited unpaired charge carriers. These currents are induced by the time-dependent variations in the local magnetic-flux density associated with the imposed change of state. They may not only lead to certain deviations of the magnetic-field distribution from textbook Meissner profiles, but also cause dissipative Joule heating, which appears to be at odds with the expected reversibility in a truly thermodynamic superconducting state. We show that these normal currents also produce a magnetocaloric cooling, which in total instantaneously and precisely compensates for the dissipated heat, thus ensuring overall energy conservation and reversibility in terms of energy. However, the time-dependent Joule heating and magnetocaloric cooling processes are spatially distinct and therefore must result in temperature inhomogeneities that only fade away towards thermodynamic equilibrium after the thermodynamic change of state has halted.**

The Meissner effect in superconductors was discovered almost a century ago<sup>1</sup>. According to this effect, an external magnetic field can be expelled by superconducting shielding currents, which, as it has later been shown, consist of Cooper pairs<sup>2</sup>. There is a consensus that at any finite temperature, some of these pairs break up and thereby create un-paired quasiparticles, so that part of the electronic system can then be regarded to behave as normal conducting. This is a central assumption of the well-known "two-fluid model"<sup>3,4</sup>. By applying an external alternating magnetic field, corresponding "normal currents" can be induced which are subject to dissipation (i.e., the generation of Joule heat), a process that is also undisputed and well-studied<sup>5</sup>. Nevertheless, a fundamental aspect has been largely overlooked: such normal currents

can also be triggered by induction even in the absence of an external electromagnetic excitation, namely simply by changing the temperature in the superconducting state, since the local magnetic field also varies over time with temperature. This raises a fundamental question: how can the existence of dissipative currents be reconciled with the thermodynamic state of superconductivity and with the reversibility of associated thermodynamic changes of state?

### Time dependent London equation

To elucidate the underlying principles at play, we start with the distribution of the local magnetic field  $\mathbf{B}(\mathbf{r})$  in the Meissner state of a superconductor that can be obtained by solving

$$-\Delta \mathbf{B}(\mathbf{r}) + \frac{\mathbf{B}(\mathbf{r})}{\lambda^2} = 0, \quad (1a)$$

as it was originally derived from the second London equation in the static limit<sup>6</sup>, with solutions adapted to the required boundary conditions. The quantity  $\lambda$  represents an effective magnetic penetration depth, which is only in the clean limit and for  $\lambda_L \gg \xi$  (where  $\lambda_L$  is the London penetration and  $\xi$  the coherence length) identical to  $\lambda_L$  associated with the density  $n_s$  of superconducting charge carriers. In the opposite limit  $\lambda_L < \xi$  and in the dirty limit,  $\lambda$  is better described by expressions provided by Pippard, which consider non-local corrections and impurities<sup>7</sup> and lead to  $\lambda > \lambda_L$ , but the general form of equation (1a) remains virtually unchanged. With increasing temperature  $T$  towards the critical temperature  $T_c$ ,  $n_s$  decreases due to the thermal breaking of Cooper pairs, leading to a rapid divergence of  $\lambda(T)$  in all cases. At finite temperature below  $T_c$ , the electronic system can therefore be thought to be composed of a superconducting ( $n_s$ ) and a normal conducting ( $n_n$ ) component, which add up to the total density  $n$  of charge carriers. This concept has been very successful in describing the superconducting state<sup>3,4</sup>, especially for alternating currents and magnetic fields<sup>5</sup>, with  $n_n$  often approximated by  $n_n \approx n(T/T_c)^4$ <sup>3</sup>.

However, if we allow for a time dependence of  $\mathbf{B}(\mathbf{r}, t)$  and of the associated current density  $\mathbf{j}(\mathbf{r}, t)$  related to  $\mathbf{B}$ , equation (1a) must be modified<sup>8-10</sup>. The total current density  $\mathbf{j}$  can then be thought of as being split into a supercurrent  $\mathbf{j}_s$  related to  $n_s$ , responsible for the Meissner magnetic-shielding effect, and a normal current  $\mathbf{j}_n$ , which is typically present only upon an external stimulus. The curl operation applied to the quasistatic version of the Maxwell equation  $\nabla \times \mathbf{B} = \mu_0 \mathbf{j} = \mu_0 (\mathbf{j}_s + \mathbf{j}_n)$  (valid for  $\mathbf{B}(\omega)$  frequencies  $\omega \ll c/R$ , where  $R$  is the size of the superconducting body and  $c$  the speed of light<sup>11</sup>), leads to a time-dependent version of equation (1a)<sup>8-10</sup>,

$$-\Delta \mathbf{B}(\mathbf{r}, t) + \frac{\mathbf{B}(\mathbf{r}, t)}{\lambda^2} = \mu_0 \nabla \times \mathbf{j}_n(\mathbf{r}, t) = \mu_0 \nabla \times \sigma \mathbf{E}(\mathbf{r}, t) = -\mu_0 \sigma \frac{\partial \mathbf{B}(\mathbf{r}, t)}{\partial t}, \quad (1b)$$

which has been successfully used to solve several time-dependent problems<sup>12-14</sup>. With the vector potential  $\mathbf{A}(\mathbf{r}, t)$  in the London gauge belonging to a solution  $\mathbf{B}(\mathbf{r}, t) = \nabla \times \mathbf{A}(\mathbf{r}, t)$  of equation (1b), it has been assumed here that the electric field  $\mathbf{E} = -\partial \mathbf{A} / \partial t$  affects  $\mathbf{j}_n$  according to Ohm's law  $\mathbf{j}_n = \sigma \mathbf{E}$  with the electrical conductivity  $\sigma$ , while its influence on  $\mathbf{j}_s$  is described by the London equation through  $\mathbf{j}_s = -\mathbf{A} / (\mu_0 \lambda^2)$ . If the variation of  $\mathbf{B}$  with time is sufficiently slow in a quasistatic limit,  $\sigma$  can be regarded as a real, frequency independent quantity and may near  $T_c$  be assumed to be close to the normal-state conductivity  $\sigma_n$ , but it can still vary with temperature (see equation (6) in the Methods Section). The choice of the actual value of  $\sigma$  does not change the main qualitative conclusions of this article as long as  $\sigma > 0$ , however. If we now allow for thermodynamic changes of state in the Meissner phase, such as the slow cooling or heating in a constant external magnetic field, the  $\mathbf{B}(\mathbf{r}, t)$  becomes time-dependent due to the temperature (and therefore time-) dependence of  $\lambda(T)$ . Consequently, the magnetic-field and current distributions can deviate from those provided by the "static" London equation (1a). In addition, the normal currents generated inevitably lead to irreversible dissipation, no matter how slow the changes of state are. Legitimate considerations have therefore been made about the reversibility in a truly thermodynamic superconducting state as treated in generally accepted models of superconductivity<sup>15-18</sup>. We are discussing here all these issues and show that the Joule heating is exactly compensated by the magnetocaloric cooling produced by the very same normal currents. However, the Joule heating profile is spatially different from the distribution of the magnetocaloric cooling power, leading to small non-equilibrium temperature gradients during such changes of state. We at first develop the underlying thermodynamics, cross check it with the result from the perspective of electrodynamics, and then generalize it to study the consequences for thermodynamic changes of state in the Meissner phase of superconductors.

### Power distribution and energy balance

We first consider the changes  $du$  in the local internal energy density  $u$  of any reversibly magnetized material with magnetization  $\mathbf{M}$  in a magnetic field  $\mathbf{H}$  upon variations of the entropy density  $s$  and the magnetic induction  $\mathbf{B} = \mu_0(\mathbf{H} + \mathbf{M})$  in terms of the first law of thermodynamics,

$$du = Tds + \mathbf{H} \cdot d\mathbf{B}. \quad (2)$$

By using  $\mathbf{H} \cdot d\mathbf{B}$  (instead of  $\mathbf{H} \cdot d\mathbf{M}$ ), we are including in  $u$  all contributions related to the magnetic field, i.e., also the magnetic energy density of empty space. To identify the relevant mechanism, we first assume complete thermal insulation of the material from the environment in an adiabatic process,  $ds = 0$ , so that  $du = \mathbf{H} \cdot d\mathbf{B}$ . If any time-dependent variation of  $\mathbf{B}(t)$  induces extended currents  $\mathbf{j}_{ind}(\mathbf{r}, t)$  in closed conducting paths according to Faraday's law of induction, these currents generate an additional "induced field"  $\mathbf{H}_{ind}(\mathbf{r}, t)$  related to  $\mathbf{j}_{ind}$  via the Maxwell equation  $\nabla \times \mathbf{H}_{ind} = \mathbf{j}_{ind}$ . The total local magnetic field  $\mathbf{H}(\mathbf{r}, t)$  can then be interpreted as the sum of the local magnetic field  $\mathbf{H}_0(\mathbf{r}, t)$  that would be present in the absence of induced currents, and  $\mathbf{H}_{ind}(\mathbf{r}, t)$ . In an extended but finite conducting body,  $\mathbf{j}_{ind}$  must be finite at its surface. The corresponding boundary condition for  $\mathbf{H}_{ind}(\mathbf{r}, t)$  is therefore  $\mathbf{H}_{ind,surf} = \mathbf{0}$  so that the total magnetic field remains continuous there. The additional change  $du_{ind}$  in the internal energy density is  $du_{ind} = \mathbf{H}_{ind} \cdot d\mathbf{B}$ . For a varying  $\mathbf{B}(\mathbf{r}, t)$  we can therefore assign an associated local power density  $p_{ind}$  to account for changes of  $u_{ind}$  with time,

$$p_{ind}(\mathbf{r}, t) = \frac{\partial u_{ind}}{\partial t} = \mathbf{H}_{ind}(\mathbf{r}, t) \cdot \frac{\partial \mathbf{B}(\mathbf{r}, t)}{\partial t}, \quad (3)$$

with  $p_{ind} = 0$  at the surface. An alternative derivation of equation (3) can be made directly from electrodynamics using Poynting's theorem  $\partial u_{ind}/\partial t = -\nabla \cdot \mathbf{S} - \mathbf{j}_{ind} \cdot \mathbf{E}$ <sup>19</sup>, applied here specifically to the present problem. With the Poynting vector  $\mathbf{S} = \mathbf{E} \times \mathbf{H}_{ind}$  and the vector identity  $\nabla \cdot \mathbf{S} = (\nabla \times \mathbf{E}) \cdot \mathbf{H}_{ind} - (\nabla \times \mathbf{H}_{ind}) \cdot \mathbf{E}$ , it yields the same result with  $\nabla \times \mathbf{E} = -\partial \mathbf{B}/\partial t$  and  $\nabla \times \mathbf{H}_{ind} = \mathbf{j}_{ind}$ . To properly account for energy conservation, the power density  $p_{ind}$  in equation (3) must be considered along with all other sources of power, such as possible internal Joule heat production, or externally supplied heat to achieve non-adiabatic reversible temperature changes in an experiment.

We now allow for such a controlled temperature change at a rate  $dT/dt$  in a constant  $\mathbf{H}_0$ . A non-zero  $\partial \mathbf{B}/\partial t$  then originates only from the varying  $\partial \mathbf{M}/\partial t = (\partial \mathbf{M}/\partial T)(dT/dt)$ . Lenz's law dictates that for any combination of signs of  $dT/dt$  and  $\partial \mathbf{M}/\partial T$ , the  $\partial \mathbf{B}/\partial t$  and  $\mathbf{H}_{ind}$  produced by the induced currents always have opposite signs, so that strictly  $p_{ind} < 0$  (see Supplementary Information, Section 1), and we may identify this energy withdrawal from the magnetized material by the currents as a magnetocaloric-cooling process<sup>20-23</sup>. At the same time, the induced currents  $\mathbf{j}_{ind}(\mathbf{r}, t)$  themselves may be subject to dissipation.

The equation (3) is a very general result and is by no means restricted to superconductors, or even to the mere presence of magnetic materials. If, as in the present case,  $\partial \mathbf{B}/\partial t$  stems from a

substance with non-zero  $\partial\mathbf{M}/\partial t$  in a constant  $\mathbf{H}_0$  alone,  $p_{ind}(\mathbf{r}, t)$  corresponds to the local magnetocaloric cooling power, leading to a real local cooling of the material. This is, e.g., the basis for the operation of certain thermomagnetic generators, where a conducting pick-up coil is placed around a paramagnet with a strongly temperature dependent magnetic susceptibility in a closed electrical circuit<sup>24</sup>. Upon repeatedly cycling the temperature, an external surplus of heat must be supplied by a heat reservoir to compensate for the magnetocaloric heat that is converted into electrical energy. In the opposite limit of  $\partial\mathbf{B}/\partial t$  related to an external alternating magnetic field  $\partial\mathbf{H}_0/\partial t$  only and in the absence of magnetized matter,  $p_{ind}(\mathbf{r}, t)$  represents the local energy withdrawal from the electromagnetic field by the induced currents. This is the case for the classic skin effect in metals, or when an empty pick-up coil in a closed resistive circuit draws energy from a varying  $\mathbf{H}_0(t)$ . It is essential to note that the power distribution in such processes is generally spatially inhomogeneous, because the Joule heat is generated near the edges of an experimental set-up, while the energy withdrawal occurs primarily in the enclosed volume.

To make the spatial power distribution more transparent, we briefly consider for simplicity an axially symmetric case of a long conducting cylinder with radius  $R$  and electrical conductivity  $\sigma$ , with magnetic fields directed along the cylinder axis  $\hat{\mathbf{z}}$ , so that we can use cylindrical coordinates and focus on the respective components  $\mathbf{B} = B_z$ ,  $j_{ind} = j_{ind,\varphi}$ ,  $\mathbf{E} = E_\varphi$ . The local Joule heating power density is

$$p_J(\mathbf{r}, t) = j_{ind}(\mathbf{r}, t)^2/\sigma. \quad (4)$$

Using the Maxwell equations  $-\partial B(r, t)/\partial t = \partial/\partial r[rE(r, t)]/r$ ,  $H_{ind}(r, t) = \int_r^R j_{ind}(r', t)dr'$  and Ohm's law  $j_{ind}(r, t) = \sigma E(r, t)$ , the local power density  $p_{ind}$  becomes with equation (3)

$$p_{ind}(\mathbf{r}, t) = (-\partial[rj_{ind}(r, t)]/\partial r) \int_r^R j_{ind}(r', t)dr' / (r\sigma). \quad (5)$$

Obviously, the  $p_J(\mathbf{r}, t)$  and  $-p_{ind}(\mathbf{r}, t)$ , expressed by  $j_{ind}(\mathbf{r}, t)$ , are not equal, so that the Joule heating profile is different from the distribution of  $p_{ind}(\mathbf{r}, t)$ . However, we show in Section 2 of the Supplementary Information that for arbitrary geometries and  $\sigma(\mathbf{r})$ , the corresponding quantities  $P_J(t)$  and  $P_{ind}(t)$  obtained by integration over the whole sample volume, exactly cancel out at any time  $t$ , thus ensuring global energy conservation.

We now return to the case of a superconductor in the Meissner state, which is the main subject of this article. Neglecting all extrinsic effects, the role of  $\mathbf{j}_{ind}(\mathbf{r}, t)$  induced by  $\partial\mathbf{B}/\partial t$  is taken

by the normal current  $\mathbf{j}_n(\mathbf{r}, t)$  in the spirit of equation (1b), which represents both the source of Joule heating and magnetocaloric cooling according to equations (4) and (5). If we have exact solutions of equation (1b) for  $\mathbf{B}(\mathbf{r}, t)$  which may differ from those of (1a), or of any other equation that correctly describes the time dependence of the Meissner effect but also leads to normal currents determined by Faraday's law of induction, the same formalism and conclusions from above apply without obvious restrictions. This is one of the central results of our article. We emphasize here that the dissipationless supercurrent  $\mathbf{j}_s(\mathbf{r}, t)$  is not caused by Faraday's law, but is, due to its quantum mechanical origin, given by its proportionality to  $-\mathbf{A}(\mathbf{r}, t)$ . Its possible time dependence is reflected in that of  $\mathbf{B}(\mathbf{r}, t)$ , which in turn provides the driving force for  $\mathbf{j}_n(\mathbf{r}, t)$ . A corresponding analogue to equation (3) for  $\mathbf{j}_s$  would represent the variation in magnetic energy density  $u_{mag} = \mathbf{B}^2/(2\mu_0)$ , with  $\partial u_{mag}/\partial t = \mathbf{B} \cdot (\partial \mathbf{B}/\partial t)/\mu_0$ .

### Numerical estimates

We first briefly examine the order of magnitude of  $\mathbf{j}_n$  that we can expect in real superconductors. We suppose the validity of equation (1b) and that we are dealing with an idealized type-I superconductor, but with material parameters similar to those of niobium with  $T_c = 9 \text{ K}$ <sup>25</sup> and an effective penetration depth  $\lambda_0 = 47 \text{ nm}$  at  $T = 0$ <sup>26</sup> with a two-fluid-like temperature dependence,  $\lambda(T)^{-2} = \lambda_0^{-2}(1 - [T/T_c]^4)$ . To account for a possible  $T$ -dependence of  $\sigma$  below  $T_c$ , we assume that it obeys a Drude-type law where  $\sigma(T)$  is proportional to  $n_n$ , i.e.,  $\propto (T/T_c)^4$ , and to a material-specific scattering time  $\tau(T)$ , the  $T$ -dependence of which we take from corresponding resistivity data where superconductivity had been quenched by a magnetic field (see Methods Section and ref. (27)). For consistency, we normalize it to a realistic value at  $T_c$ ,  $\sigma(T_c) = \sigma_n = 1.8 \times 10^9 (\Omega\text{m})^{-1}$ , which we estimate from the thermal conductivity  $\kappa \approx 400 \text{ W/(Km)}$  given in ref. (28) at  $T_c$  using the Wiedemann-Franz law,  $\sigma_n = \kappa/(LT)$ , with  $L = 2.44 \times 10^{-8} \text{ W}\Omega\text{K}^{-2}$ . However, as we shall see below, significant measurable thermal effects are only expected to occur close to  $T_c$ , so that the knowledge of the exact temperature dependence below  $T_c$  is not crucial in this respect.

During field cooling a corresponding infinitely long superconducting cylinder with radius  $R = 6\lambda_0$  in a  $B_0 = \mu_0 H_0$  well below the critical field  $B_c$  at a realistic cooling rate  $dT/dt = -0.05 \text{ K/s}$  across the critical temperature, the  $B_z(r, t)/B_0$  as obtained by numerically solving equation (1b) (see Methods Section) is virtually indistinguishable from the corresponding static solution given by equation (1a) and plotted in Fig. 1a. Pronounced deviations would only occur in a regime where  $\mathbf{j}_n$  becomes comparable to the order of magnitude of  $\mathbf{j}_s$ . The dimensionless,  $T$ -

independent parameter  $\epsilon = (\mu_0 \sigma_n \lambda(0)^2 / T_c) (dT/dt)$  is related to the ratio of the leading prefactors of  $\mathbf{j}_n(\mathbf{r})$  and  $\mathbf{j}_s(\mathbf{r})$  as derived from the respective analytical solution of equation (1a) and given in equations (12) and (13) of the Supplementary Information. In our model superconductor,  $\epsilon \approx 3 \times 10^{-14}$  only, which is a typical order of magnitude for existing superconductors. We have also tentatively assumed extremely high hypothetical  $\sigma_n$  values between  $2.6 \times 10^{20} (\Omega\text{m})^{-1}$  ( $\epsilon \approx 0.004$ ) and  $2.6 \times 10^{23} (\Omega\text{m})^{-1}$  ( $\epsilon \approx 4$ ) and plotted the resulting  $B_z(r, t)/B_0$  in Figs. 1b-1f for comparison. However, the crossover criterion  $\epsilon \approx 1$  in Fig. 1d is by many orders of magnitudes unreachable for existing superconductors under realistic experimental field-cooling or warming conditions, except perhaps in an extremely narrow region around  $T_c$ , so that possible effects of a finite  $\mathbf{j}_n$  on  $\mathbf{B}(r, t)$  are probably not directly measurable. We can nevertheless conclude from this important consideration that the solutions of equation (1a) serve as an excellent approximation for the quantitative modelling of slowly varying magnetic fields and currents in real superconducting systems, and we will therefore use the corresponding analytic solutions in the following.

On this basis, we provide in Section 3 of the Supplementary Information explicit formulae for  $p_J(r, t)$  and  $p_{ind}(r, t)$  for a cylinder geometry and in the realistic limit  $\epsilon \ll 1$ , where not only  $\mathbf{B}(r)$  but also all relevant current densities are virtually indistinguishable from the static solutions associated with equation (1a). In Figs. 2a-2d, we show the resulting  $p_J(r, t)$  and  $p_{ind}(r, t)$  for our model superconductor and for small particle sizes at temperatures close to  $T_c$ , locally reaching several Watts/m<sup>3</sup>. The powers  $P_J$  and  $-P_{ind}$ , integrated over the cylinder cross section, strongly increase towards  $T_c$  with  $(\partial\lambda/\partial T)^2$  and cylinder radius  $R$  as illustrated in Fig. 2e. Very near  $T_c$ ,  $P_J$  is expected to grow rapidly as  $R^8$  (see Supplementary Information, equation (18)). If  $T$  approaches the critical regime, it is in principle a critical exponent that determines the divergence of  $\lambda(T)$  and hence the rate  $\partial\mathbf{B}(r, t)/\partial t$ , although a corresponding correction with respect to the simple two-fluid approximation has not been considered relevant<sup>29</sup>.

### Thermal effects

The spatial separation of heated and cooled zones, as given by equations (4), (5) and shown Figs. 2a-2d, must result in the formation of certain temperature gradients, the extent and magnitude of which depend on the rate of heat diffusion. The regions of pronounced local heat generation where the normal currents  $\mathbf{j}_n(\mathbf{r}, t)$  are strongest are always qualitatively closer to the edge of the superconductor than the zones where the cooling power dominates. We illustrate



this also in Fig. 2f, where the relevant length scales are plotted in dimensionless units that neither depend on the choice of material parameters nor on a particular temperature protocol. For small particles or close to  $T_c$  where  $R/\lambda(T)$  is small, the heated zone with  $p_J > |p_{ind}|$  covers a significant area of the cross section, while it is squeezed towards the edge with increasing  $R/\lambda(T)$ , i.e., for large sample dimensions or low temperatures, respectively. According to our estimates and numeric simulations of the heat-diffusion equation, using a thermal conductivity  $\kappa \approx 400$  W/(Km)<sup>28</sup> and a heat capacity per volume  $C \approx 2.7 \times 10^4$  J/(Km<sup>3</sup>)<sup>30</sup> (see Methods Section), temperature gradients in submillimeter-sized samples during slow field-cooling processes are small, i.e., for a  $dT/dt = -0.05$  K/s only in the  $\mu$ K range immediately below  $T_c$  and even less below, and they may therefore have gone unnoticed until now. Nevertheless, they might be accessible in precise ac calorimetry-type experiments near  $T_c$ <sup>31,32</sup> where the  $dT/dt$  of corresponding temperature oscillations can be made substantially larger since both  $p_J$  and  $p_{ind}$  are proportional to  $(dT/dt)^2$  (see Supplementary Information, equations (11)-(16)), and in wide samples as the total Joule heat increases strongly with  $R$  as  $R^8$  (Fig. 2e).

Because  $p_J$  is largest near  $T_c$  where the heated regions near the circumference of the superconductor expand towards the center due to the diverging  $\lambda(T)$  as we have shown it in Figs. 2 and particularly in Fig. 2f,  $n_s$  must become depleted (together with a further local increase of  $\lambda$ ) or even suppressed in such a heated edge region close enough to  $T_c$ . Therefore, when the superconductor is cooled from the normal state, superconductivity is expected to develop initially in the center region and will be possible only for effective radii  $R' < R$  since  $P_J$  increases strongly with increasing  $R$ . It should then spread very rapidly into the bulk as the temperature is further reduced, while the reverse scenario must occur as the superconductor is heated. However, it may prove challenging to provide experimental evidence for this, given that a broadening of the transition due to geometric and material-related issues may mask a related effect to some extent.

It remains to be seen whether the energy balance discussed here has implications for other areas of research on superconductors, where the dissipation of induced normal currents plays a prominent role. Finally, it should be noted that the mathematical concepts described in this article are not restricted to superconductors but can be directly applied to other conducting materials with a temperature-dependent magnetic susceptibility, such as metallic ferromagnets.



## References

1. Meissner, W. & Ochsenfeld, R. Ein neuer Effekt bei Eintritt der Supraleitfähigkeit, *Naturwissenschaften* **21**, 787 (1932).
2. Bardeen, J., Cooper, L. N., & Schrieffer, J.R. Theory of Superconductivity, *Phys. Rev.* **108**, 1175 (1957).
3. Gorter, C. J. The two fluid model for superconductors and Helium II, in: *Progress in low temperature physics I*, Ch. 1 (Elsevier, North Holland, Amsterdam, 1955).
4. Bardeen, J. Two-Fluid Model of Superconductivity, *Phys. Rev. Lett.* **1**, 399 (1958).
5. For a review, see Anlage, S. M. Microwave Superconductivity, *IEEE J. of Microwaves* **1**, 389 (2021).
6. London, F. & London, H. The Electromagnetic equations of the Supraconductor, *Proc. R. Soc. Lond. Ser. A* **149**, 71 (1935).
7. Pippard, A. B. An experimental and theoretical study of the relation between magnetic field and current in a superconductor, *Proc. R. Soc. Lond. Ser. A* **216**, 547 (1953).
8. Gor'kov, L. P. & Kopnin, N. B., Vortex motion and resistivity of type-II superconductors in a magnetic field, *Sov. Phys.-Usp.* **18**, 496 (1976).
9. Refai, T. F. & Saif, A. G. Electromagnetic Fields and Power Losses for Slabs, *Phys. Stat. Sol. (b)* **166**, 201 (1991).
10. Kogan, V. G. Time-dependent London approach: Dissipation due to out-of-core normal excitations by moving vortices, *Phys. Rev. B* **97**, 094510 (2018).
11. Landau, L. D. & Lifshitz, E. M. *Electrodynamics of Continuous Media*, Ch. 7 (Pergamon, New York, 1984).
12. Kogan, V. G. & Prozorov, R. Anisotropic time-dependent London approach: Application to the ac response in the Meissner state, *Phys. Rev. B* **102**, 184514 (2020).
13. Kogan, V. G. & Ichioka, M. Vortex Cores in Narrow Thin-Film Strips, *J. Phys. Soc. Jpn.* **89**, 094711 (2020).
14. Kogan, V. G. & Nakagawa, N. Dissipation of moving vortices in thin films, *Phys. Rev. B* **105**, L020507 (2022).
15. Hirsch, J. E. On the reversibility of the Meissner effect and the angular momentum puzzle, *Annals of Physics* **373**, 230 (2016).
16. Nikulov, A. The Law of Entropy Increase and the Meissner Effect, *Entropy* **24**, 83 (2022).
17. Szeftel, J., Sandeau, N. & Ghantous, M. A. An observable prerequisite for the existence of persistent currents, *Eur. Phys. J. B* **92**, 67 (2019).
18. Koizumi, H. Reversible superconducting-normal phase transition in a magnetic field: The energy-momentum balance including the velocity field of the Berry connection from many-body wave functions, *Phys. Scr.* **99**, 015952 (2024).
19. Poynting, J. H. On the Transfer of Energy in the Electromagnetic Field, *Philos. Trans. R. Soc. London* **175**, 343 (1884).
20. Warburg, E. Magnetische Untersuchungen. Über einige Wirkungen der Coërcitivkraft, *Ann. Phys.* **249**, 141 (1881).

21. Weiss, P. & Piccard, A. Le phénomène magnétocalorique, *J. Phys. (Paris), 5th Ser.* **7**, 103 (1917).
22. Debye, P. Einige Bemerkungen zur Magnetisierung bei tiefer Temperatur, *Ann. Phys.* **386**, 1154 (1926).
23. Giauque, W. F. A Thermodynamic Treatment of Certain Magnetic Effects. A Proposed Method of Producing Temperatures Considerably Below 1° Absolute, *J. Am. Chem. Soc.* **49**, 1864 (1927).
24. For a review, see: Dzekan, D., Waske, A., Nielsch, K. & Fähler, S. Efficient and affordable thermomagnetic materials for harvesting low grade waste heat, *APL Mater.* **9**, 011105 (2021), and the references therein.
25. French, R. A., Intrinsic Type-2 superconductivity in pure niobium, *Cryogenics* **8**, 301 (1968).
26. Maxfield, B. W. & McLean, W. L. Superconducting Penetration Depth of Niobium, *Phys. Rev.* **139**, A 1515 (1965).
27. Webb, G. W. Low-Temperature Electrical Resistivity of Pure Niobium, *Phys. Rev.* **181**, 1127 (1969).
28. Koechlin, F. & Bonin, B. Parametrization of the niobium thermal conductivity in the superconducting state, *Supercond. Sci. Technol.* **9**, 453 (1996).
29. Kiometzis, M., Kleinert, H. & Schakel, A.M.J. Critical Exponents of the Superconducting Phase Transition, *Phys. Rev. Lett.* **73**, 1975 (1994).
30. Chou, C., White, D. & Johnston, H. L. Heat capacity in the normal and superconducting states and critical field of niobium, *Phys. Rev.* **109**, 788 (1958).
31. Sullivan, P. F. & Seidel, G. Steady-State, ac-Temperature Calorimetry, *Phys. Rev.* **173**, 679 (1968).
32. For a review, see Gmelin, E. Classical temperature-modulated calorimetry: A review, *Thermochimica Acta* **304/305**, 1 (1997).

## Figures

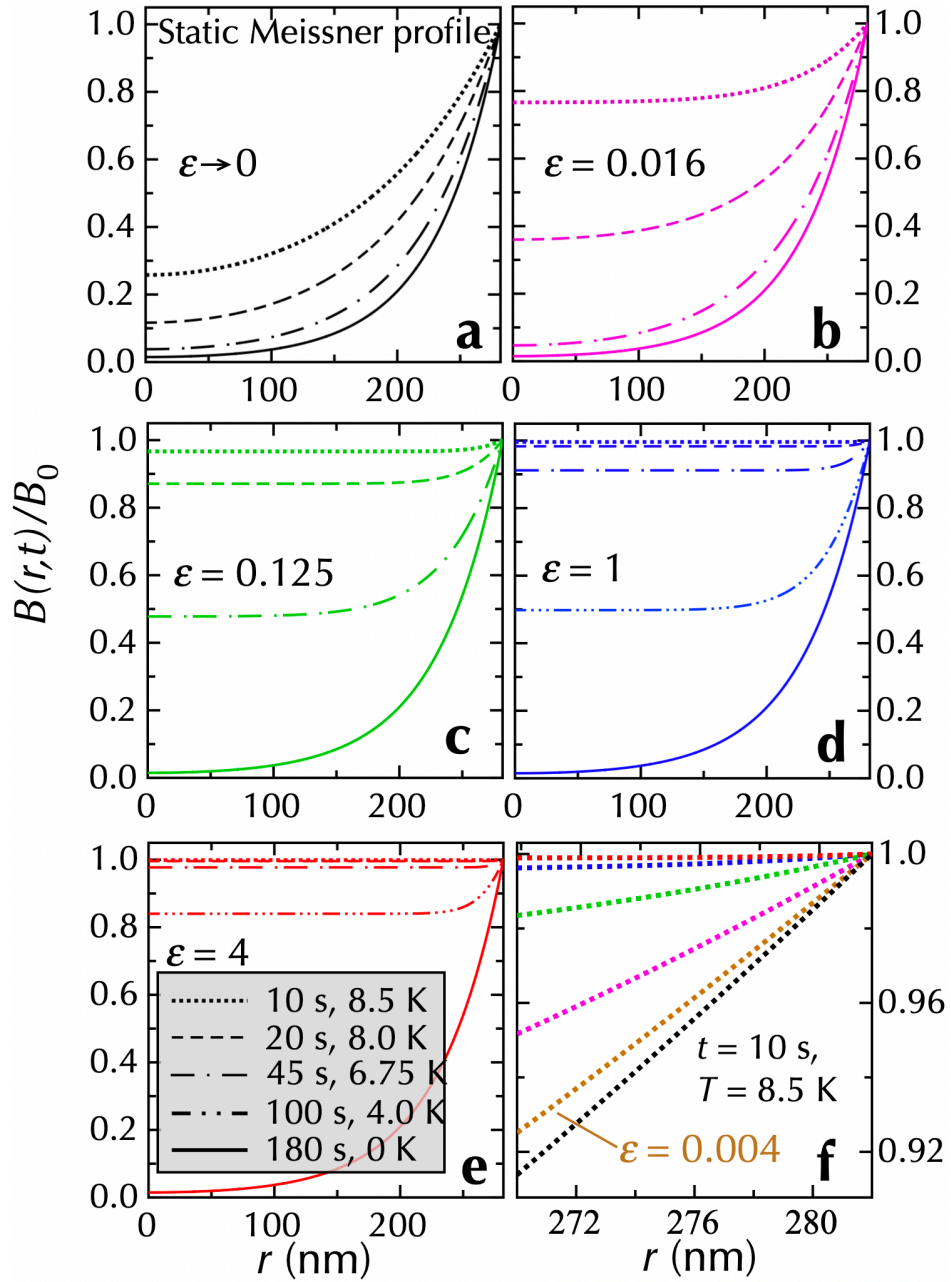


**Fig. 1: Magnetic-field distributions  $B(r, t)/B_0$  obtained by numerically solving equation (1b) for a type-I superconducting cylinder with Radius  $R = 6\lambda_0 = 282$  nm and the model parameters as described in the text, at times  $t = 10$  s, 20 s, 45 s, 100 s (for  $\epsilon = 1$  and 4 only) and 180 s, respectively, after entering the superconducting state at  $T_c = 9$  K with  $dT/dt = -0.05$  K/s. a, For the chosen model superconductor with  $\epsilon \approx 3 \times 10^{-14}$ ,  $B(r, t)/B_0$  is virtually indistinguishable from the static Meissner profile,  $\epsilon \rightarrow 0$ . b-e, Corresponding data for  $\epsilon$  around unity. f: Expanded view of the data near the edge of the cylinder for  $t = 10$  s. All hypothetical dynamic profiles for  $\epsilon > 0$  would relax to the corresponding static Meissner profiles ( $\epsilon = 0$ ) on a time scale  $\mu_0 \sigma \lambda^2$  <sup>10</sup> proportional to  $\epsilon$  after a thermodynamic change of state has stopped.**

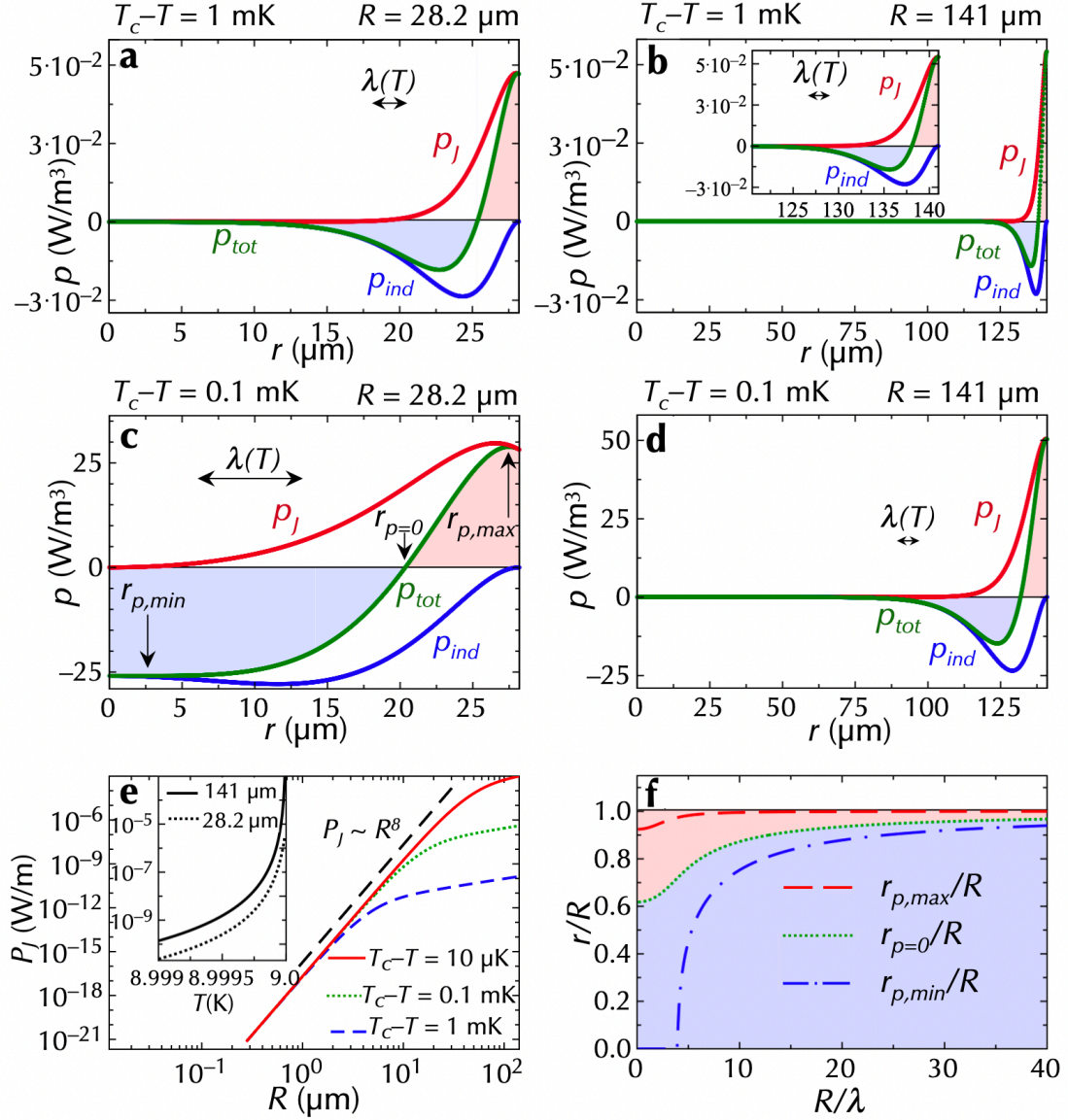


**Fig. 2: Local and integrated power densities for the model type-I superconductor as described in the text. a-d,** Local power densities  $p_J(r, t)$ ,  $p_{ind}(r, t)$  and  $p_{tot}(r, t) = p_J(r, t) + p_{ind}(r, t)$  for  $R = 600\lambda_0$  (28.2  $\mu\text{m}$ ) and  $3000\lambda_0$  (141  $\mu\text{m}$ ), respectively, each at  $t = 20$  ms ( $T_c - T = 1$  mK), and 2 ms ( $T_c - T = 0.1$  mK) after entering the superconducting state with  $dT/dt = -0.05$  K/s in  $\mu_0 H_0 = 0.1$  T. The respective magnetic penetration depths  $\lambda(T)$  are indicated with arrows. We have marked  $r_{p,max}$ ,  $r_{p=0}$ , and  $r_{p,min}$  in Fig. 2c, where the total local power density  $p_{tot}$  reaches its maximum, zero, or minimum value, respectively. **e,** Integrated power  $P_J(t) = -P_{ind}(t)$  per unit length of the cylinder as a function of  $R$  close to the critical temperature, with an  $R^8$  dependence as indicated by the straight dashed line. The inset illustrates the strong variation of  $P_J$  near  $T_c$ . **f,** Resulting values in dimensionless units as functions of  $R/\lambda(T)$ . In all these figures, the light red and light blue coloring schemes symbolize local heating and local cooling, respectively.

## **Methods**

### **Modelling the dc electrical conductivity of the normal carriers below $T_c$**

The temperature dependence of the dc electrical conductivity  $\sigma$  of the normal carriers inserted in equation (1b) was treated as follows: We assumed that  $\sigma(T)$  obeys a Drude-type law where  $\sigma$  is proportional to  $n_n$ , i.e.,  $\propto (T/T_c)^4$ , and to a material-specific scattering time  $\tau(T)$ , the  $T$ -dependence of which we took from corresponding resistivity data of niobium reported in ref. (27), where superconductivity was quenched by a magnetic field. This leads to

$$\frac{\sigma(T)}{\sigma_n(T_c)} \approx \frac{(T/T_c)^4}{0.1829 + 3.950 \times 10^{-2}(T/T_c)^2 + 0.7776(T/T_c)^3} \quad (6)$$

and is roughly proportional to  $(T/T_c)^2$ . In the numerical procedure, equation (6) was used, however.

### **Numerical procedures**

To numerically solve equation (1b) and the thermal diffusion equation mentioned in the main text, we used the software Maple 2024 by Maplesoft, Waterloo, Canada. The thermal gradients obeying the heat-diffusion equation,  $\partial T(\mathbf{r}, t)/\partial t - \kappa \Delta T(\mathbf{r}, t)/C = p_{tot}(\mathbf{r}, t)/C$  (with  $\kappa$  the thermal conductivity and  $C$  the heat capacity per volume) could alternatively be estimated by using the fact that the thermal diffusivity  $\kappa/C$  of metallic superconductors around  $T_c$  is sufficiently large ( $\kappa/C \approx 0.02 \text{ m}^2/\text{s}$ )<sup>28,30</sup> so that the temperature compensation across the steepest power gradient along  $p_{tot}(\mathbf{r}, t)$  is fast enough to approach quasi-stationary conditions for reasonably slow changes of the thermodynamic state. Then, the  $\partial T(\mathbf{r}, t)/\partial t$  becomes negligibly small compared to the other terms, and therefore  $\Delta T(\mathbf{r}, t) \approx -p_{tot}(\mathbf{r}, t)/\kappa$  holds over extended parts of the cylinder volume, the solutions of which also provide useful estimates of the temperature distribution. The  $p_{tot}(\mathbf{r}, t) = p_J(\mathbf{r}, t) + p_{ind}(\mathbf{r}, t)$  for the limiting case  $\epsilon \ll 0$  can be included here, for which analytical solutions are given in the Supplementary Information, equations (11) – (16).

The corresponding Maple worksheets are available on reasonable request.

**Acknowledgments** We thank to S.M. Anlage and to V.G. Kogan for useful comments and discussions, and to A. Drake for preparing graphic animations.

**Correspondence** should be addressed to A. Schilling

## Supplementary Information

1. List of cases with sign combinations of  $\frac{\partial B}{\partial t}$  and  $H_{ind}$  implying that  $p_{ind} < 0$ .

$\partial M/\partial T$	$dT/dt$	$\partial B/\partial t$	$H_{ind}$	$p_{ind} = H_{ind}\partial B/\partial t$
$> 0$	$> 0$	$> 0$	$< 0$	$< 0$
$> 0$	$< 0$	$< 0$	$> 0$	$< 0$
$< 0$	$> 0$	$< 0$	$> 0$	$< 0$
$< 0$	$< 0$	$> 0$	$< 0$	$< 0$

For a superconductor in the Meissner state,  $\partial M/\partial T > 0$ .

2. Proof of  $P_{ind} + P_J = 0$  for arbitrary geometries and  $\sigma(\mathbf{r})$

The local Joule heating power due to the induced currents  $\mathbf{j}_{ind}(\mathbf{r}, t)$  is

$$p_J(\mathbf{r}, t) = \frac{j_{ind}(\mathbf{r}, t)^2}{\sigma(\mathbf{r})}, \quad (1)$$

while the magnetic field produced by them is given by the Maxwell equation

$$\nabla \times \mathbf{H}_{ind}(\mathbf{r}, t) = \mathbf{j}_{ind}(\mathbf{r}, t). \quad (2)$$

As outlined in equation (3) of the main article, the power density  $p_{ind}(\mathbf{r})$  is given in general by

$$p_{ind}(\mathbf{r}, t) = \mathbf{H}_{ind}(\mathbf{r}, t) \cdot \frac{\partial \mathbf{B}(\mathbf{r}, t)}{\partial t}. \quad (3)$$

Because  $\mathbf{j}_{ind}$  is finite at the surface of an extended finite conducting body, the corresponding boundary condition for  $\mathbf{H}_{ind}(\mathbf{r}, t)$  is  $\mathbf{H}_{ind, surf} = \mathbf{0}$  so that the total magnetic field  $\mathbf{H} = \mathbf{H}_0 + \mathbf{H}_{ind}$  remains continuous and  $p_{ind} = 0$  at the surface. With the Maxwell equation

$$\frac{\partial \mathbf{B}(\mathbf{r}, t)}{\partial t} = -\nabla \times \mathbf{E}(\mathbf{r}, t) = -\nabla \times \frac{\mathbf{j}_{ind}(\mathbf{r}, t)}{\sigma(\mathbf{r})}, \quad (4)$$

we have

$$p_{ind}(\mathbf{r}, t) = -\mathbf{H}_{ind}(\mathbf{r}, t) \cdot \left\{ \nabla \times \frac{\mathbf{j}_{ind}(\mathbf{r}, t)}{\sigma(\mathbf{r})} \right\}. \quad (5)$$

The total power density  $P_{ind} + P_J$ , integrated over the whole sample volume then becomes

$$P_{ind} + P_J = \int_{vol} d\mathbf{r} [p_{ind}(\mathbf{r}, t) + p_J(\mathbf{r}, t)] = \int_{vol} d\mathbf{r} \left[ -\mathbf{H}_{ind}(\mathbf{r}, t) \cdot \left\{ \nabla \times \frac{\mathbf{j}_{ind}(\mathbf{r}, t)}{\sigma(\mathbf{r})} \right\} + \frac{j_{ind}(\mathbf{r}, t)^2}{\sigma(\mathbf{r})} \right]. \quad (6)$$

With the use of the vector identity

$$\nabla \cdot (\mathbf{H}_{ind}(\mathbf{r}, t) \times \frac{\mathbf{j}_{ind}(\mathbf{r}, t)}{\sigma(\mathbf{r})}) = (\nabla \times \mathbf{H}_{ind}(\mathbf{r}, t)) \cdot \frac{\mathbf{j}_{ind}(\mathbf{r}, t)}{\sigma(\mathbf{r})} - \mathbf{H}_{ind}(\mathbf{r}, t) \cdot \left\{ \nabla \times \left( \frac{\mathbf{j}_{ind}(\mathbf{r}, t)}{\sigma(\mathbf{r})} \right) \right\}, \quad (7)$$

the boundary condition  $\mathbf{H}_{ind, surf} = \mathbf{0}$ , and equation (2), we obtain

$$P_{ind} + P_J = \int_{vol} d\mathbf{r} \left[ \nabla \cdot (\mathbf{H}_{ind}(\mathbf{r}, t) \times \frac{\mathbf{j}_{ind}(\mathbf{r}, t)}{\sigma(\mathbf{r})}) - (\nabla \times \mathbf{H}_{ind}(\mathbf{r}, t)) \cdot \frac{\mathbf{j}_{ind}(\mathbf{r}, t)}{\sigma(\mathbf{r})} + \frac{\mathbf{j}_{ind}(\mathbf{r}, t)^2}{\sigma(\mathbf{r})} \right] \quad (8)$$

$$= \int_{vol} d\mathbf{r} \left[ \nabla \cdot (\mathbf{H}_{ind}(\mathbf{r}, t) \times \frac{\mathbf{j}_{ind}(\mathbf{r}, t)}{\sigma(\mathbf{r})}) \right] = \int_{surface} d\mathbf{n} \cdot (\mathbf{H}_{ind}(\mathbf{r}, t) \times \frac{\mathbf{j}_{ind}(\mathbf{r}, t)}{\sigma(\mathbf{r})}) = 0. \quad (9)$$

### 3. Explicit expressions for cylindrical superconductors in the Meissner state

Explicit expressions for thermodynamic changes of state of a superconductor in the Meissner state and in a constant external magnetic field  $\mathbf{H}_0$  can be obtained in the limit  $\partial T/\partial t \ll T_c/(\mu_0 \sigma_n \lambda_0^2)$  ( $\epsilon \ll 1$ ) which is always fulfilled for existing superconductors in a realistic experiment (see main article text). The resulting magnetic-field distribution is then virtually indistinguishable from that of a static London-like profile, which is for a long cylinder with radius  $R$  in cylindrical coordinates

$$B(r, t) = \mu_0 H_0 \frac{I_0\left(\frac{r}{\lambda}\right)}{I_0\left(\frac{R}{\lambda}\right)}. \quad (10)$$

We are using here and below the modified Bessel functions of the first kind  $I_0(x)$  and  $I_1(x)$ ,  $\lambda(T(t))$  the temperature (and therefore time dependent) effective penetration depth, and  $\sigma$  the normal-state electrical conductivity that we assume to be spatially constant. With

$$\frac{\partial B(r, t)}{\partial t} = \mu_0 H_0 \frac{\partial \lambda}{\partial T} \frac{dT}{dt} \frac{-r I_0\left(\frac{R}{\lambda}\right) I_1\left(\frac{r}{\lambda}\right) + R I_0\left(\frac{r}{\lambda}\right) I_1\left(\frac{R}{\lambda}\right)}{\lambda^2 I_0\left(\frac{R}{\lambda}\right)^2} \quad (11)$$

and  $r j_n(r, t) = -\sigma \int_0^r r' \frac{\partial B(r', t)}{\partial t} dr'$  with  $j_n(0, t) = 0$  we obtain

$$j_n(r, t) = -\mu_0 H_0 \sigma \frac{\partial \lambda}{\partial T} \frac{dT}{dt} \frac{[-r I_0\left(\frac{r}{\lambda}\right) + 2\lambda I_1\left(\frac{r}{\lambda}\right)] I_0\left(\frac{R}{\lambda}\right) + R I_1\left(\frac{R}{\lambda}\right) I_1\left(\frac{r}{\lambda}\right)}{\lambda I_0\left(\frac{R}{\lambda}\right)^2}, \quad (12)$$

whereas the supercurrent density is

$$j_s(r) = j_{tot}(x) - j_n(r, t) \approx j_{tot}(x) = -\frac{H_0}{\lambda} \frac{I_1\left(\frac{r}{\lambda}\right)}{I_0\left(\frac{R}{\lambda}\right)}. \quad (13)$$

The resulting local Joule power density is

$$p_J(r, t) = \frac{j_n(r, t)^2}{\sigma}. \quad (14)$$



The  $H_{ind}(r) = \int_r^R j_n(r')dr'$  becomes

$$H_{ind}(r, t) = \mu_0 H_0 \sigma \frac{\partial \lambda}{\partial T} \frac{dT}{dt} \left( \frac{2\lambda I_0(\frac{r}{\lambda}) I_0(\frac{R}{\lambda}) + R I_0(\frac{r}{\lambda}) I_1(\frac{R}{\lambda}) - r I_0(\frac{R}{\lambda}) I_1(\frac{r}{\lambda})}{I_0(\frac{R}{\lambda})^2} - 2\lambda \right), \quad (15)$$

which can be used to calculate the local magnetocaloric cooling power with equation (11),

$$p_{ind}(r, t) = H_{ind}(r, t) \frac{\partial B(r, t)}{\partial t}. \quad (16)$$

The total Joule power  $P_J = -P_{ind}$ , integrated over the cross section of the cylinder is with  $A_0 = I_0(\frac{R}{\lambda})$  and  $A_1 = I_1(\frac{R}{\lambda})$

$$P_J(t) = \frac{\pi R \sigma (\mu_0 H_0 \frac{\partial \lambda}{\partial T} \frac{dT}{dt})^2}{3\lambda^2 A_0^4} \times \quad (17)$$

$$[A_0^4(R^3 - 12\lambda^2 R) + A_0^3 A_1(24\lambda^3 - 10\lambda R^2) + A_0^2 A_1^2(22\lambda^2 R - 4R^3) + 12A_0 A_1^3 \lambda R^2 + 3A_1^4 R^3].$$

In the limit  $T \rightarrow T_c$  this amounts per unit length of the cylinder to

$$P_J(T \rightarrow T_c) = \frac{11}{768} \pi R^8 \sigma (\mu_0 H_0 \frac{dT}{dt})^2 \lim_{T \rightarrow T_c} \left( \frac{\frac{\partial \lambda(T)}{\partial T}}{\lambda(T)^3} \right)^2. \quad (18)$$